Theoretical evaluation of Young's moduli of polymers

Sung Y. Hong and Miklos Kertesz
Department of Chemistry, Georgetown University, Washington, D.C. 20057
(Received 4 December 1989)

The elastic (Young's) moduli of *trans*-polyethylene (PE), *trans*-polyacetylene (PA), and two types (*cis*-transoid and *trans*-cisoid) of *cis*-PA were studied using three theoretical schemes. The analytical method derived in this work not only predicts fairly good values for the moduli when the spectroscopic force constants are used but also gives information on geometrical changes upon longitudinal deformation. With this method, the moduli of *trans*-PE and *trans*-PA were calculated from the spectroscopic force-constant matrices to be 286 and 372 GPa, respectively. The moduli of two types of *cis*-PA are similar in value and about half of the value for *trans*-PA. Although the semiempirical modified neglect of diatomic overlap solid-state theory predicted higher moduli of the polymers compared with experimentally determined values, it provides reasonable values when combined with force-constant scaling. The moduli of the polymers were analyzed and discussed in terms of geometrical changes of the carbon chain and branched hydrogens. The following qualitative conclusions emerged from this study: (a) the Young's modulus is strongly influenced by not only the force constants but also the conformation of polymers, (b) side groups may have large contributions, and (c) bond-angle deformations do not always dominate Young's modulus.

SCALING FORCE CONSTANTS AND THE CALCULATION OF YOUNG'S MODULUS

During the past several decades many attempts have been made to evaluate the elastic (Young's) modulus, Y, of polymers experimentally[1-12] and theoretically[13-23] because it is one of the important mechanical properties of polymers. The experimental techniques range from mechanical stress-strain measurements,[1,2] x-ray diffraction,[3-6] and infrared experiments[7] on stressed polymer crystals, and inelastic neutron scattering methods[8] to Raman studies of the longitudinal acoustic vibrational mode.[9-12] Aside from the issue of sample impurities and imperfections, the microscopic value of Y, which determines the ultimate elastic modulus of the polymer, remains uncertain. The experimental data are scattered ranging from 240 to 358 GPa for *trans*-polyethylene (PE) and from 18 to 80 GPa for polypropylene. For theoretical evaluations several valence force fields[13-18] and quantum-chemical calculations[19-23] have been tried. Treloar[13] derived a simple formula for the modulus of a linear polymer on the basis of diagonal force constants and applied it to polyethylene and nylon 66, and obtained 182 and 196 GPa, respectively. Shimanouchi *et al.*[14] attributed the low modulus of polyethylene predicted by Treloar to his simple valence force field and extended the method using the Urey-Bradley force field and obtained $Y=340$ GPa. Intermediate Y values were predicted by other force field calculations.[15-18] A quantum-chemical approach was first applied to the calculation of Young's modulus of polymers by Boudreaux[19] using a version of the complete neglect of differential overlap (CNDO/2) method. Subsequently, Christ *et al.*,[20] Dewar *et al.*,[21] and Karpfen[22] made quantum-chemical calculations of the modulus of *trans*-PE, and these calculated values lie between 300 and 500 GPa. In general, quantum-chemical calculations predict significantly larger values compared with the experimentally determined ones. Recently, Suhai[23] included electron correlations effects with second-order Moller-Plesset perturbation theory to predict a reasonable modulus for *trans*-PE.

The aim of this paper is to develop a reliable microscopic method for the calculation of the elastic modulus of polymers. The elastic modulus, Y, for one-dimensional crystals can be defined in terms of the second derivative of the potential energy E of a unit cell with respect to the translation vector c, as follows:

$$Y=cA^{-1}(d^2E/dc^2)\ , \tag{1}$$

where A is the cross-sectional area perpendicular to c. Therefore, information on the energy surface around the equilibrium geometry enables one to calculate Y. Such information can be obtained through spectroscopic measurements and theoretical calculations since the potential-energy surface is related to the force constants, K_{ij}, at the equilibrium geometry:

$$K_{ij}=\partial^2E/\partial Q_i\partial Q_j\ , \tag{2}$$

where $E=E(Q_i)$ is the energy of a unit cell, and Q_i are the coordinates, internal or Cartesian, of the atoms of the system. Such calculations are becoming possible using quantum-chemical methods as the calculation of the total energy for polymers and solids with several atoms per repeat unit is becoming a routine task.

Any microscopic theory of the elastic constant has to solve two problems: (a) how to correct for systematic deficiencies of the $E(Q_i)$ energy surface, and (b) how the particular elastic constants can be expressed in terms of the various K_{ij} force constants. The latter question is related to the distribution of the elastic deformation among the different internal coordinates. This distribution is of

importance, because those force constants that couple strongly to the deformation need to be determined accurately.

Let us analyze, as an example, a simple model for calculating the Young's modulus of a zig-zag equidistant chain, as illustrated in Fig. 1. The way the elongation of the unit cell, δc, is coupled to the change of the internal coordinates, δQ_i (δr and $\delta\theta$), is crucial in determining the associated energy change and consequently, the Young's modulus. Since $K_{rr} > K_{\theta\theta}$, it seems that the angle deformation dominates the calculated value of Y. Our analysis in this paper shows that this is an oversimplification. The reason, simply put, is that even though the energy change is quadratically related to the deformations:

$$\delta E \approx \tfrac{1}{2}K_{rr}\delta r^2 + \tfrac{1}{2}K_{\theta\theta}\delta\theta^2 + \cdots , \tag{3}$$

the smaller δr value is accompanied by a larger K_{rr} force constant. The crucial issue is how δQ_i values are coupled to the elongation δc. Force constants involving the side group R in Fig. 1, for instance, play a small but sometimes not negligible role, as we will show.

Hartree-Fock calculations systematically overestimate the stretching and bending force constants, and lead to too high vibrational frequencies.[24] Correcting force constants by systematic scaling has become a matter of routine in molecular quantum chemistry since the work of Pulay and his coworkers.[25] Extension to polymers is straightforward.[26] In the present work we have employed a hierarchy of schemes to find out what approximations can be made that will allow this scaling in the calculation of the Young's modulus of a polymer.

Table I displays the schemes we developed here. Scheme I is the direct method which calculates Y from the quantum chemistry based energy surface around an optimized translation vector. The total-energy calculations are based on the modified neglect of diatomic overlap (MNDO) approach as extended to polymers using translational symmetry.[21,27] The schemes can be applied to any other Hamiltonian, including *ab initio* ones. Scheme II is the analytical method which calculates and analyzes the modulus from force constants obtained either quantum chemically or spectroscopically. In scheme III, the geometrical changes are predicted by a quantum-chemical method and these deformations are connected with the best available force constants. This combination results in a semianalytical method for the calculation of Y. By developing and comparing these schemes, we obtain an insight into the quality of the Young's modulus predictions.

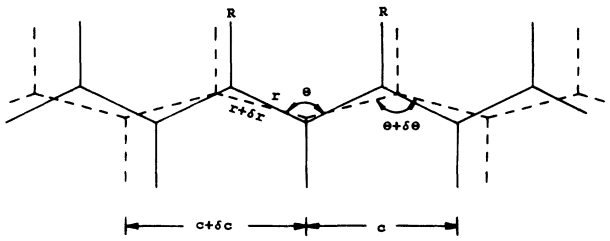

FIG. 1. A simple model for calculating the Young's modulus of a zig-zag equidistant chain (solid line represents the chain at equilibrium and dashed line after elongation of the chain.).

DERIVATION OF THE EXPRESSION FOR THE ELASTIC MODULUS

Since the potential energy E of a unit cell is dependent on the (internal) coordinates Q_i of the constituent atoms in the cell, the differential of E can be given in the first-order approximation by

$$dE = \sum_i (\partial E/\partial Q_i) dQ_i \quad \text{for } i = 1,2,\ldots,N , \tag{4}$$

where N is the number of total coordinates in a unit cell.

TABLE I. Schemes used in this study for calculating Young's moduli of polymers.

Schemes	Brief description	Comments
I. Direct method	Search the minimum of the energy surface by optimizing geometric parameters for constituent atoms while the translation vector is varied.	Pure quantum-chemical method is applied.
II. Analytical method	Variation of geometrical parameters upon longitudinal deformation as well as Young's modulus are analytically evaluated from the force constant matrix.	Theoretically or empirically determined force constants can be used, scaling is possible.
III. Semianalytical method	Use force-constant matrix to evaulate Young's modulus by Eq. (6) in the text while adapting the quantum-mechanically determined geometrical deformation.	Same as scheme II.

Division of Eq. (4) by dc followed by differentiating with respect to c yields

$$\frac{d^2E}{dc^2}=\sum_i\sum_j(\partial^2E/\partial Q_i\partial Q_j)(dQ_i/dc)(dQ_j/dc)+\sum_i(\partial E/\partial Q_i)(d^2Q_i/dc^2)\ . \tag{5}$$

Since all $(\partial E/\partial Q_i)$ are negligible around the equilibrium geometry, Eq. (5) reduces to

$$E''=\sum_i\sum_j K_{ij}Q_i'Q_j'\ , \tag{6}$$

where a prime denotes the first derivative with respect to a translation vector c and a double prime denotes the second derivative. K_{ij} is the equilibrium force constant, which includes the interactions of the intercell coordinates Q_i/Q_j as well as the corresponding intracell coordinates in the following manner:

$$K_{ij}=\sum_n F_{ij}(n)\ , \tag{7}$$

where $F_{ij}(n)$ is the force constant between coordinates Q_i and Q_j separated by n unit cells and $F_{ij}(0)$ is the intracell force constant. Since K_{ij}'s are constant within the harmonic approximation, a set of Q_i' variables fully determine Young's modulus. The optimal Q_i' values correspond to the minimal change of energy upon longitudinal deformation. However, translational symmetry puts geometrical constraints on the selection of a set of such optimal Q_i' values. Since the length of a unit cell is a function of the internal coordinates, $c=f_m(Q_1,Q_2,\ldots,Q_N)$, the following relationship can be established:

$$dc=\sum_i(\partial f_m/\partial Q_i)dQ_i \quad \text{for } m=1,2,\ldots,M\ , \tag{8}$$

which are constraints on the Q_i's for the Young's modulus calculation of translationally symmetrical systems and where M is the number of constraints and $m\geq 1$. It is convenient to express the constraints as a function of a set of Q_i' variables which describe the deformations of the various Q_i coordinates upon longitudinal deformation. Division of Eq. (8) by dc yields

$$1=\sum_i(\partial f_m/\partial Q_i)Q_i'\ . \tag{9}$$

Let us define a function Ω and introduce Lagrangian multipliers ϵ_m to accommodate the geometrical constraints for minimizing E''. Then,

$$\Omega=\sum_i\sum_j K_{ij}Q_i'Q_j'-\sum_m\epsilon_m\left[\sum_i\left[\frac{\partial fm}{\partial Q_i}\right]Q_i'-1\right]\ . \tag{10}$$

For the minimum value of E'', set the derivatives of Ω with respect to Q_i' and ϵ_m to zero. This leads to Eqs (9) and (11),

$$2\sum_j K_{ij}Q_j'+\sum_m\epsilon_m(\partial f_m/\partial Q_i)=0\ . \tag{11}$$

There are $N+M$ linear equations to be solved, which lead to a form of

$$\underline{A}\cdot\mathbf{X}=\mathbf{B}\ , \tag{12}$$

where $\underline{A}$ is a coefficient matrix that consists of force constants and $\partial f_m/\partial Q_i$ geometrical coupling coefficients:

$$\underline{A}=\begin{bmatrix} K_{11} & K_{12} & \cdots & K_{1N} & \partial f_1/\partial Q_1 & \cdots & \partial f_M/\partial Q_1 \\ K_{21} & K_{22} & \cdots & K_{2N} & \partial f_1/\partial Q_2 & \cdots & \partial f_M/\partial Q_2 \\ \vdots & \vdots & & \vdots & \vdots & & \vdots \\ K_{N1} & K_{N2} & \cdots & K_{NN} & \partial f_1/\partial Q_N & \cdots & \partial f_M/\partial Q_N \\ \partial f_1/\partial Q_1 & \partial f_1/\partial Q_2 & \cdots & \partial f_1/\partial Q_N & 0 & \cdots & 0 \\ \vdots & \vdots & & \vdots & \vdots & & \vdots \\ \partial f_m/\partial Q_1 & f_M/\partial Q_2 & \cdots & \partial f_M/\partial Q_N & 0 & \cdots & 0 \end{bmatrix}\ , \tag{13a}$$

$$\mathbf{X}=\begin{bmatrix} Q_1' \\ Q_2' \\ \vdots \\ Q_N' \\ \epsilon_1 \\ \epsilon_2 \\ \vdots \\ \epsilon_M \end{bmatrix},\quad \mathbf{B}=\begin{bmatrix} 0 \\ 0 \\ \vdots \\ 0 \\ 1 \\ 1 \\ \vdots \\ 1 \end{bmatrix}\ . \tag{13b}$$

TABLE II. Optimized geometrical parameters (geometrical parameters for polymers are defined in Fig. 2) for *trans*-polyethylene (PE), *trans*-polyacetylene (PA), and two types of *cis*-PA using MNDO solid-state method.

			cis-PA	
Q_i[a]	*Trans*-PE	*Trans*-PA	Transoid	Cisoid
R_1	1.543	1.357	1.358	1.462
R_2	1.543	1.462	1.459	1.357
θ	114.00	124.86	128.89	128.38
r_H	1.114	1.096	1.097	1.097
ϕ_H	109.07	119.57	115.68	112.18
τ_H	57.85			
c	2.587	2.500	2.275	2.304

[a]Bond lengths and angles are in units of Å and degree, respectively.

The solution of **X** can be simply expressed by

$$\mathbf{X}=\underline{A}^{-1}\cdot\mathbf{B}\ . \tag{14}$$

Therefore, from the known force-constant matrix and the geometry of a system, Young's modulus can be evaluated according to Eqs. (2), (5), and (14).

CALCULATIONS AND RESULTS

The geometries of the polymers referred to in this study were optimized by the MNDO solid-state method[21,27] and are given in Table II. (See also Fig. 2.) The unit cells of the polymers were taken as the unit with two C atoms to allow comparison of contributions from different coordinates. Energy surfaces of the polymers were calculated with 11 k points in k space for *trans*-PE and *cis*-PA's and 21 k points for *trans*-PA. We have included 12 neighboring unit cells on each side for *trans*-PE, 13 for *trans*-PA, and 15 for *cis*-PA's, the maximum numbers allowed by the present version of the program. In this study we used the optimized geometries. For the effective cross-sectional area A we used the following x-ray-based values: 18.24 Å^2 for *trans*-PE (Ref. 28) and 15.52 Å^2 for *trans*-PA (Ref. 29). The effective areas of *cis*-PA were assumed to be the same as that of *trans*-PA. Three schemes are listed in Table I, which were used to evaluate the Young's modulus for the four polymers studied in this paper.

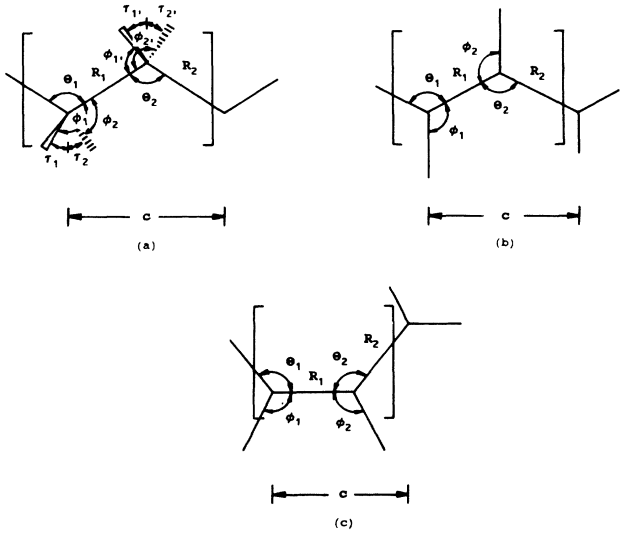

FIG. 2. Geometrical parameters of the polymers used in this study: (a) *trans*-polyethylene, (b) *trans*-polyacetylene, and (c) *cis*-polyacetylene ($R_1<R_2$, *cis*-transoid and $R_1>R_2$, *trans*-cisoid).

Scheme I is the direct method which numerically calculates Young's modulus from the energy surfaces. E'' is calculated numerically by changing c by $\delta c=\pm 0.01$ Å around its optimized value while the other geometric parameters are correspondingly reoptimized. The calculated ratios of geometry changes to longitudinal deformation are summarized in Table III, which are the numerical approximations on the Q_i's. The calculated Young's moduli of the polymers are given in the first row of Table IV. Klei and Stewart[27] obtained 360 GPa for *trans*-PE using the MNDO method using slightly different lattice summation and k-space sampling. As expected, the predicted values are greater than the experimentally determined values listed in Table IV. An analysis of the other two schemes will shed light on this overestimation problem. It should be mentioned, however, that the mechanical stress-strain measurements for polyacetylenes produced rather low values probably owing to the low crystallinity and the morphology of the sample.

In scheme II, Young's moduli of the polymers were analytically evaluated from the force-constant matrices as described in the previous section and the MNDO optimized geometries. To compare the quantum-chemical calculations and spectroscopic methods, force constants determined either quantum-chemically or spectroscopically were employed. The MNDO force constants were numerically calculated from the gradient for internal coordinates, obtained by shifting geometrical parameters in steps of 0.005 Å for bond lengths and 0.1° for bond an-

TABLE III. The variation of geometrical parameters of *trans*-polyethylene (PE), *trans*-polyacetylene (PA), and two types of *cis*-PA upon longitudinal deformation.

			Cis-PA	
	Trans-PE	*Trans*-PA	Transoid	Cisoid
	MNDO solid-state method			
$\delta R_1/\delta c$	0.245	0.186	0.112	0.194
$\delta R_2/\delta c$	0.245	0.316	0.074	0.039
$\delta\theta/\delta c$[a]	0.702	0.850	0.741	0.735
$\delta r_H/\delta c$	−0.010	0.016	0.031	0.027
$\delta\phi_H/\delta c$[a]	−0.193	−0.389	−0.272	−0.315
$\delta\tau_H/\delta c$[a]	−0.089			
	Analytical method using spectroscopic force constants			
dR_1/dc	0.292	0.263	0.150	0.193
dR_2/dc	0.292	0.314	0.075	0.066
$d\theta/dc$[a]	0.607	0.751	0.707	0.720
dr_H/dc	0.000	0.000	0.000	0.000
$d\phi_H/dc$[a]	−0.126	−0.541	−0.458	−0.400
$d\tau_H/dc$[a]	0.000			

[a]The units are rad/Å.

TABLE IV. Young's moduli, Y (GPa), of *trans*-polyethylene (PE), *trans*-polyacetylene (PA), and two types of *cis*-PA.

Y (GPa)	*Trans*-PE	*Trans*-PA	*Cis*-PA Transoid	*Cis*-PA Cisoid
This work[a] I	368.8	590.5	309.0	325.4
II[b]	286.4	372.6	170.1[c]	188.2[c]
III[b]	298.6	384.3	178.7[c]	190.9[c]
Other quantum-chemical studies	297,[d] 405,[e] 493.5,[f] 406,[g] 345,[g] 362,[h] 303[h]			
Force-field studies	182,[i] 340,[j] 256.4,[l] 320,[m] 315.5[n]	300–400[k]	100[k]	
X-ray	240,[o] 255[p]			
Neutron Scattering	329[q]			
Raman study of LAM	340,[r] 358,[s] 290,[u] 280[v]	450[t]		
Mechanical stress-strain measurements	288[w]	100[x]	30–40[x]	

[a]I, II, and III refer to results obtained by schemes I, II, and III, respectively.
[b]Spectroscopic force-constant matrix is used; force constants of *trans*-PE and *trans*-PA are taken from Refs. 30 and 31, respectively.
[c]The same force constants are used as those of trans-PA.
[d]Taken from Ref. 19.
[e]Taken from Ref. 20.
[f]Taken from Ref. 21.
[g]Taken from Ref. 22.
[h]Taken from Ref. 23.
[i]Taken from Ref. 13.
[j]Taken from Ref. 14.
[k]Quoted in Ref. 2.
[l]Taken from Ref. 16.
[m]Taken from Ref. 17.
[n]Taken from Ref. 18.
[o]Taken from Ref. 4.
[p]Taken from Ref. 6.
[q]Taken from Ref. 8.
[r]Taken from Ref. 9.
[s]Taken from Ref. 10.
[t]Derived in this study from the slope of the calculated LAM taken from Ref. 31.
[u]Taken from Ref. 11.
[v]Derived in this study from the experimental dispersion curve taken from Ref. 32.
[w]Taken from Ref. 1.
[x]Taken from Ref. 2.

gles. Certain coupling constants between bond angles are not separable from the diagonal force constants due to the translational symmetry. For instance, the θ_1/θ_2 coupling is included (in a 50-50 ratio) in the θ_1/θ_1 and θ_2/θ_2 diagonal terms. The calculated MNDO force-constant matrices of the polymers are tabulated in Tables V–VII. The spectroscopic force-constant matrices were taken from the Ref. 30 for *trans*-PE and from Ref. 31 for *trans*-PA. These were calculated to include the interactions with the next-nearest-neighboring unit cells by summing up the coupling constants between the cells according to Eq. (7). Since spectroscopic force constants for *cis*-PA's were not available, the force constants of *trans*-PA were adapted. The spectroscopic force-constant matrices used in this study are in Tables VIII and IX. The geometrical constraints for each polymer are given in the Appendix.

This scheme reproduced the same values for the moduli within 0.2% and the same geometrical changes in size and direction as the one obtained in scheme I when the MNDO force-constant matrices were used. This scheme also allowed us to calculate the distribution of the moduli based on internal coordinates as shown in Table X.

The moduli of the polymers predicted using spectroscopic force constants are shown together with their decomposition in Table XI. The value for *trans*-PE is fairly good compared to the experimental values. As can be seen in Tables X and XI, large contributions come from the diagonal terms. The contributions of angle de-

TABLE V. MNDO force-constant matrix K_{ij} of *trans*-polyethylene. Units are mdyn/Å for bond stretching and coupling constants, mdyn for stretch-bend coupling constants, and mdyn Å for other constants. Geometrical parameters are defined in Fig. 2.

Coordinates	R_1	R_2	θ_1	θ_2	r_{H_1}	ϕ_{H_1}	τ_{H_1}	r_{H_2}
R_1	6.298							
R_2	0.923	6.298						
θ_1	0.510	0.115	1.561					
θ_2	0.510	0.115	0.000	1.561				
r_{H_1}	0.320	0.320	−0.143	0.000	5.887			
ϕ_{H_1}	0.374	−0.210	0.148	0.148	0.003	1.073		
τ_{H_1}	−0.005	0.292	0.248	0.000	−0.005	0.073	0.862	
r_{H_2}	0.320	0.320	−0.143	0.000	0.236	−0.118	0.215	5.887
ϕ_{H_2}	0.374	−0.210	0.148	0.148	−0.118	0.183	−0.171	0.003
τ_{H_2}	−0.005	−0.292	0.248	0.000	0.215	−0.171	0.390	−0.005
r_{H_3}	0.320	0.320	0.000	−0.143	0.013	0.001	−0.002	0.006
ϕ_{H_3}	0.374	−0.210	0.148	0.148	0.001	−0.004	0.011	0.011
τ_{H_3}	−0.005	−0.292	0.000	0.248	−0.002	−0.011	0.011	−0.020
r_{H_4}	0.320	0.320	0.000	−0.143	0.006	0.011	−0.020	0.013
ϕ_{H_4}	0.374	−0.210	0.148	0.148	0.011	0.073	0.024	0.001
τ_{H_4}	−0.005	−0.292	0.000	0.248	−0.020	0.024	0.033	−0.002

	ϕ_{H_2}	τ_{H_2}	r_{H_3}	ϕ_{H_3}	τ_{H_3}	r_{H_4}	ϕ_{H_4}	τ_{H_4}
ϕ_{H_2}	1.073							
τ_{H_2}	0.073	0.862						
r_{H_3}	0.011	−0.020	5.887					
ϕ_{H_3}	0.073	0.024	0.003	1.073				
τ_{H_3}	0.024	0.033	−0.005	0.073	0.862			
r_{H_4}	0.001	−0.002	0.236	−0.118	0.215	5.887		
ϕ_{H_4}	−0.004	−0.011	−0.118	0.183	−0.171	0.003	1.073	
τ_{H_4}	−0.011	0.011	0.215	−0.171	0.390	−0.005	0.073	0.862

formation of the two *trans* polymers is comparable with that of bond-length deformation while in *cis*-PA's, the former is dominant. It should be noted that coupling of C—C—H angle deformation with the carbon-chain deformation yields significantly negative contributions to the moduli of the polymers.

Our goal of using scheme III was to investigate the possibility of using force-constant scaling in connection with a quantum-chemical prediction and analysis of Young's modulus. In this scheme, the theoretically computed ratios of geometrical changes to the longitudinal deformation are combined with scaled force constants to predict Young's modulus using Eq. (6) directly. In the present study, the spectroscopic force constants were employed instead of scaled ones. The results are quite close to the ones of scheme II as shown in Table IV.

TABLE VI. MNDO force-constant matrix, K_{ij} of *trans*-polyacetylene. Units are the same as in Table V. Geometrical parameters are defined in Fig. 2.

Coordinates	R_1	R_2	θ_1	θ_2	r_{H_1}	ϕ_{H_1}	r_{H_2}	ϕ_{H_2}
R_1	10.885							
R_2	1.700	7.477						
θ_1	0.563	0.165	1.520					
θ_2	0.563	0.165	0.000	1.520				
r_{H_1}	0.462	0.368	−0.332	0.000	6.294			
ϕ_{H_1}	0.408	−0.399	0.320	0.320	0.029	1.186		
r_{H_2}	0.462	0.368	0.000	−0.332	0.021	0.000	6.294	
ϕ_{H_2}	0.408	−0.399	0.320	0.320	0.000	0.085	0.029	1.186

TABLE VII. MNDO force-constant matrices, K_{ij}, of two forms of *cis*-polyacetylenes. Units are the same as in Table V. Geometrical parameters are defined in Fig. 2.

Coordinates	R_1	R_2	θ_1	θ_2	r_{H_1}	ϕ_{H_1}	r_{H_2}	ϕ_{H_2}
			Cis-transoid polyacetylene					
R_1	10.862							
R_2	1.712	7.574						
θ_1	0.634	0.199	1.699					
θ_2	0.634	0.199	0.000	1.699				
r_{H_1}	0.433	0.352	−0.337	0.000	6.266			
ϕ_{H_1}	0.378	−0.463	0.252	0.252	0.083	1.279		
r_{H_2}	0.433	0.352	0.000	−0.337	0.027	−0.012	6.266	
ϕ_{H_2}	0.378	−0.463	0.252	0.252	−0.012	0.126	0.083	1.279
			Trans-cisoid polyacetylene					
R_1	7.485							
R_2	1.745	10.885						
θ_1	0.607	0.194	1.652					
θ_2	0.607	0.194	0.000	1.652				
r_{H_1}	0.375	0.420	−0.354	0.000	6.275			
ϕ_{H_1}	0.381	−0.460	0.260	0.260	0.011	1.274		
r_{H_2}	0.375	0.420	0.000	−0.354	0.025	−0.016	6.275	
ϕ_{H_2}	0.381	−0.460	0.260	0.260	−0.016	0.118	0.011	1.274

TABLE VIII. Spectroscopic force-constant matrix K_{ij} of *trans*-polyethylene. Units are the same as in Table V. Geometrical parameters are defined in Fig. 2.

Coordinates	R_1	R_2	θ_1	θ_2	r_{H_1}	ϕ_{H_1}	r_{H_2}	ϕ_{H_2}
R_1	4.427							
R_2	0.128	4.427						
θ_1	0.351	0.351	0.901					
θ_2	0.351	0.351	0.186	0.901				
r_{H_1}	0.000	0.000	0.000	0.000	4.456			
ϕ_{H_1}	0.261	−0.004	0.124	−0.058	0.000	0.666		
r_{H_2}	0.000	0.000	0.000	0.000	0.016	0.000	4.456	
ϕ_{H_2}	0.261	−0.004	0.124	−0.058	0.000	−0.016	0.000	0.666
τ_H [a]	0.000	0.000	0.000	0.000	0.000	0.000	0.000	0.000
r_{H_3}	0.000	0.000	0.000	0.000	0.000	0.000	0.000	0.000
ϕ_{H_3}	0.261	−0.004	−0.058	0.124	0.000	−0.048	0.000	0.312
r_{H_4}	0.000	0.000	0.000	0.000	0.000	0.000	0.000	0.000
ϕ_{H_4}	0.261	−0.004	−0.058	0.124	0.000	0.312	0.000	−0.048
$\tau_{H'}$ [b]	0.000	0.000	0.000	0.000	0.000	0.000	0.000	0.000
	τ_H [a]	r_{H_3}	ϕ_{H_3}	r_{H_r}	ϕ_{H_4}	$\tau_{H'}$ [b]		
τ_H [a]	0.550							
r_{H_3}	0.000	4.456						
ϕ_{H_3}	0.000	0.000	0.666					
r_{H_4}	0.000	0.016	0.000	4.456				
ϕ_{H_4}	0.000	0.000	−0.016	0.000	0.666			
$\tau_{H'}$ [b]	0.000	0.000	0.000	0.000	0.000	0.550		

[a]Defined as the sum of τ_{H_1} and τ_{H_2}.

[b]Defined as the sum of $\tau_{H_1'}$ and $\tau_{H_2'}$.

TABLE IX. Spectroscopic force-constant matrix K_{ij} of *trans*-polyacetylene. Units are the same as in Table V. Geometrical parameters are defined in Fig. 2.

Coordinates	R_1	R_2	θ_1	θ_2	r_{H_1}	ϕ_{H_1}	r_{H_2}	ϕ_{H_2}
R_1	6.291							
R_2	0.814	5.141						
θ_1	0.382	0.131	0.763					
θ_2	0.382	0.131	0.280	0.763				
r_{H_1}	0.000	0.000	0.000	0.000	4.995			
ϕ_{H_1}	0.418	−0.041	0.144	0.173	0.000	0.559		
r_{H_2}	0.000	0.000	0.000	0.000	0.000	0.000	4.995	
ϕ_{H_2}	0.418	−0.041	0.173	0.144	0.000	0.060	0.000	0.559

ANALYSIS USING THE DIAGONAL APPROXIMATION

For the purpose of analysis we introduce a diagonal approximation: $K_{ij}=\delta_{ij}K_{ij}$, where δ_{ij} is the Kronecker δ. Then we obtain for PE,

$$R_1'=R_2'=(\partial c/\partial R)/K_{RR}B\ , \tag{15a}$$

$$\theta_1'=\theta_2'=(\partial c/\partial\theta)/K_{\theta\theta}B\ , \tag{15b}$$

$$Y=2c(K_{RR}R'^2+K_{\theta\theta}\theta'^2)/A=2c/AB\ , \tag{15c}$$

where c is a length of a unit cell, A is an effective area, and

$$B=(\partial c/\partial R)^2/K_{RR}+(\partial c/\partial\theta)^2/K_{\theta\theta}\ , \tag{15d}$$

and for PA's (both *trans* and *cis* isomers)

$$R_1'=2(\partial c/\partial R_1)/K_{R_1R_1}D\ , \tag{16a}$$

$$R_2'=2(\partial c/\partial R_2)/K_{R_2R_2}D\ , \tag{16b}$$

$$\theta_1'=\theta_2'=(\partial c/\partial\theta)/K_{\theta\theta}D\ , \tag{16c}$$

$$Y=c(K_{R_1R_1}R_1'^2+K_{R_2R_2}R_2'^2+2K_{\theta\theta}\theta'^2)/A$$
$$=2c/AD\ , \tag{16d}$$

where

$$D=2(\partial c/\partial R_1)^2K_{R_1R_1}+2(\partial c/\partial R_2)^2K_{R_2R_2}$$
$$+(\partial c/\partial\theta)^2/K_{\theta\theta}\ . \tag{16e}$$

This approximation provides a rough estimate for the

TABLE X. Analysis of Young's moduli Y (in GPa), using the analytical method (scheme II) with MNDO force constants. The Y is decomposed according to deformations of local coordinates.

	Trans-PE	*Trans*-PA	*Cis*-PA Transoid	*Cis*-PA Cisoid
Total	369.1	591.5	308.6	325.4
decomposition[a]				
R_1/R_1	53.4	60.9	20.1	41.8
R_2/R_2	53.4	120.8	6.1	2.5
θ_1/θ_1	109.2	176.7	136.5	132.4
θ_2/θ_2	109.2	176.7	136.5	132.4
r_H/r_H	0.3	0.4	1.7	1.3
ϕ_H/ϕ_H	22.8	57.7	27.9	37.4
τ_H/τ_H	3.9			
R_1/R_2	15.7	32.3	4.2	3.9
R_1/θ	49.7	57.4	30.9	51.3
R_2/θ	11.2	28.6	6.4	3.3
R_1/ϕ_H	−20.1	−19.0	−6.8	−13.8
R_2/ϕ_H	11.3	31.6	5.5	3.4
θ/ϕ_H	−45.7	−136.1	−59.7	−71.4
θ_{τ_H}	−17.7			
Residual terms	12.5	3.5	−0.7	0.9

[a] Q_i/Q_j indicates the contribution arising from the force constant $K_{Q_iQ_j}$ associated with the coupling of the local deformation coordinates Q_i and Q_j.

TABLE XI. The analysis of Young's moduli Y (in GPa), using the analytical method (scheme II) with spectroscopic force constants. The total Y is decomposed according to deformations of local coordinates.

	Trans-PE	*Trans*-PA	*Cis*-PA Transoid	*Cis*-PA Cisoid
Total	286.4	372.6	170.1	188.2
decomposition[a]				
R_1/R_1	53.7	69.8	20.7	28.5
R_2/R_2	53.7	81.8	4.2	4.1
θ_1/θ_1	47.0	69.2	55.9	58.7
θ_2/θ_2	47.0	69.2	55.9	58.7
r_H/r_H	0.0	0.0	0.0	0.0
ϕ_H/ϕ_H	6.0	52.7	34.4	26.6
τ_H/τ_H	0.0			
R_1/R_2	3.1	21.6	2.7	3.1
θ_1/θ_2	19.4	50.8	41.0	43.1
R_1/θ	35.3	48.5	23.7	10.8
R_2/θ	35.3	19.9	4.1	10.8
R_1/ϕ_H	−10.9	−38.3	−16.8	1.9
R_2/ϕ_H	0.2	4.5	0.8	−6.6
θ/ϕ_H	−5.7	−82.9	−60.2	−54.3
θ/τ_H	0.0			
Residual terms	2.3	5.7	3.7	2.8

[a] Same as in Table X.

modulus and is useful to understand the behavior of geometrical changes upon longitudinal deformation. From the preceding equations for a given system, the geometrical change is proportional to $(\partial c/\partial Q_i)$ and the inverse of the corresponding force constant. Therefore, larger contribution from the deformation of a coordinate is expected even if the force constant is smaller since its contribution to Y is proportional to the square of the geometrical change. According to the equations for PA's, the existence of a coordinate with greater force constant enforces larger geometrical changes of the other coordinates because D becomes smaller, leading to a larger modulus.

DISCUSSION

Our analytical method predicts a fairly good value for the Young's modulus for *trans*-PE compared to values obtained from experiments and other force-field studies. Especially, it is noticeable that the predicted value shows an excellent agreement with the value from strain-stress measurements of Barham and Keller,[1] and with the corrected value of Strobl and Eckel,[11] who took weak interlamellar forces into account in interpreting Raman spectra of the longitudinal acoustic mode (LAM). Since the work of Treloar,[13] Young's moduli of several polymers have been calculated using various valence force fields. However, the previous force-field methods could not give any information on geometrical changes upon longitudinal deformation and, thus, on the distribution of the modulus in terms of geometrical changes. The advantage of our analytical method is that such information can be obtained including the effect of side groups. On the experimental side Wool and Boyd[7] investigated geometrical changes for polypropylene through ir frequency shifts with stress.

To our knowledge, there is no reliable result for Young's modulus of crystalline PA's. Our best calculated value for Y is 373 GPa. This predicted modulus of trans-PA is lower by 80 GPa than the value obtained by us from the slope of calculated longitudinal acoustic phonon dispersion curve of Takeuchi *et al.*[1] and is within the range of unpublished values quoted in Ref. 2. Our best predicted moduli of two forms of *cis*-PA (170 and 188 GPa) are higher than the corresponding unpublished result (100 GPa). These values are subject to an uncertainty, since the same force-constant matrices and the effective areas were used for the *cis*-conformers as those for *trans*-PA.

Young's moduli of the polymers calculated by unscaled MNDO solid-state method are higher than the predicted values from the spectroscopic force constants, but comparable with the other quantum-chemical methods. It should be noted that Dewar *et al.*[21] predicted a much higher value for Young's modulus for *trans*-PE although they also used the MNDO Hamiltonian. Their calculation does not allow the complete relaxation of carbon atoms upon longitudinal deformation, explaining why their value is the highest among all calculated Young's moduli. The modulus of *trans*-PE calculated by the *ab initio* method[22,23] depends on the choice of the basis set. Slater-type-orbital (STO)-3G basis set predicts higher values and extended basis sets give slightly lower values than the MNDO solid-state method.

It is interesting that the moduli calculated as described in scheme III are comparable with the values obtained from spectroscopic force constants since this sheds light on the possibility of using scaled force constants in the calculation of Young's modulus. This stems from the fact that the geometrical changes, upon longitudinal deformation, predicted by MNDO method are quite similar as seen in Table III to the values obtained from the spectroscopic force constants.

It is predicted in this study that *trans*-PA has a Young's modulus higher than *trans*-PE by about 100 GPa and a modulus about twice that of *cis*-PA's. In what follows we attempt to explain these differences. We used for the cross-sectional area A values from x-ray diffraction studies, which in itself gives rise to about 15% difference between the Young's moduli of polyethylene and polyacetylene.

Let us define the total contribution of a single Q_i' to the modulus as sum of the contribution of the diagonal term and a half of all contributions of coupling terms arising from Q_i'. Then, from Table XI, the total contribution of single-bond deformations of *trans*-PE amounts to 140.5 GPa and that of angle deformations to 145.8 GPa. In *trans*-PA, deformation of double bonds contributes 95.7 GPa, and of single bonds and angles of the carbon chain 104.8 and 182.0 GPa, respectively. In *cis*-transoidal (*trans*-cisoidal) PA, each deformation contributes 34.2 (7.8) GPa for double bonds, 8.0 (35.9) GPa for single bonds, and 136.6 (144.2) GPa for angles. Angle deformation in *trans*-PE and *trans*-PA, in spite of its much smaller force constants, contributes to the modulus as much as do bond-length deformations. This comes from the larger deformation of the former as expected from the diagonal approximation. The double bond of *trans*-PA makes the modulus higher than that of *trans*-PE partially since the force constant is larger which induces the larger changes of the single bond and the angle and, thereby, the modulus. We used the same force constants for *trans*- and *cis*-PA's because the data for *cis*-PA's are not available. Young's moduli of *cis*-PA's are around half of that of *trans*-PA in spite of the same force-constant values since, in *cis*-PA's, only the contribution of angle deformation is considerable. This is due to the difference in the geometries of the *trans* versus *cis* conformations and is reflected in the smaller values of $(\partial c/\partial R_i)/(\partial c/\partial\theta)$ of *cis* conformers. For *cis*-PA's this results in smaller geometrical changes in bond lengths and, thereby, leads to a smaller Young's modulus.

The effect of branched hydrogens on a modulus of a carbon chain has not been discussed yet because of the failure of previous valence force-field methods to include the coordinates of the hydrogen atoms. We have found in this study that deformation of hydrogen coordinates occurs through coupling with deformations of the chain and only C—C—H angle deformation is significant. The analysis showed that the direct contribution of the hydrogens to the modulus is negligible. However, through coupling with bond length and angle deformations, hydro-

gens have an overall lowering effect on Young's modulus, especially for polyacetylenes. That is, although the direct total contribution is −2.2 GPa for *trans*-PE, −5.6 GPa for *trans*-PA, and −3.7 (−2.9) GPa for transoid (cisoid) of *cis*-PA, it lowers the contribution of the chain deformation indirectly by as much as 8.3 for *trans*-PE, 60.6 GPa for *trans*-PA, and 38.5 (30.5) GPa for *cis*-transoidal (*trans*-cisoidal) PA. In order to check the effects of the hydrogen atoms on Young's modulus, we have performed the calculation of the modulus without taking into account force constants associated with hydrogen atoms using scheme II. The results are 294.6 GPa for *trans*-PE, 424.9 GPa for *trans*-PA, and 214.7 GPa for transoidal and cisoidal PA's. By correcting these values by the previously listed H contributions, we get values very close to the results by the complete calculations including H contributions.

CONCLUSION

A new analytical method for the calculation of the elastic (Young's) modulus for polymers was developed. Since this method expresses the modulus in terms of the force-constant matrix and internal coordinates of a system, it can give information on geometrical changes upon longitudinal deformation. Based on the spectroscopic force-constant matrix and the MNDO optimized geometry of the polymers investigated, the Young's modulus was predicted to be 286 GPa for *trans*-PE and 373 GPa for *trans*-PA. The higher modulus of *trans*-PA is attributed to the greater deformations of single-bond distances and bond angles along the carbon chain due to the existence of double bonds. Bond-angle deformation of the carbon chain of *trans*-PE and *trans*-PA, in spite of its much smaller force constants, contributes to the modulus about as much as do bond-length deformations due to larger deformation of the former.

The Young's moduli of the two *cis* forms of PA mostly originate from the deformation of bond angles while the contributions of the slant bonds are negligible. This results in both forms of *cis*-PA being about half as strong as *trans*-PA as far as Young's modulus is concerned. C—C—H angle deformations are significant and they lower the contributions of the carbon-chain deformations through coupling.

Unscaled MNDO solid-state calculations yield higher moduli of the polymers because of the overestimation of force constants inherent in Hartree-Fock based methods, in general. Therefore, it is recommended from the comparison of the schemes used in this work that quantum-mechanical force constants be scaled down, as is usually done for vibrational analysis, to predict a better value for Young's modulus when spectroscopic force constants are not available. For instance, the scaled MNDO force constants[33] for *trans*-PE yield the prediction of 330 GPa for Young's modulus using our analytical method.

ACKNOWLEDGMENTS

This work was supported by the U.S. Air Force Office of Scientific Research under Grant No. AFOSR-89-0229, and the Camille and Henry Dreyfus Foundation. Stimulating discussions with Dr. R. Baughmann are gratefully acknowledged. We also thank Dr. C. X. Cui for providing us his scaled MNDO polyethylene force constants.

APPENDIX

Below is a summary of the geometrical constraints for the systems considered (all bond distances in Å and all bond angles in radians).

1. *Trans*-polyethylene

Since $c = 2R_1 \sin(\theta_1/2)$,

$$\partial c/\partial R_1 = 2\sin(\theta_1/2) = 1.677$$

and

$$\partial c/\partial \theta_1 = R_1 \cos(\theta_1/2) = 0.840$$

from the predicted geometry. Also $R_1 = R_2$, and $\theta_1 = \theta_2$. Therefore,

$$1.677R_1' + 0.840\theta_1' = 1 , \quad \text{(A1)}$$

$$1.677R_1' + 0.840\theta_2' = 1 , \quad \text{(A2)}$$

$$1.677R_2' + 0.840\theta_2' = 1 . \quad \text{(A3)}$$

2. *Trans*-polyacetylene

Since $c^2 = R_1^2 + R_2^2 - 2R_1R_2\cos\theta_1$,

$$\partial c/\partial R_1 = (R_1 - R_2\cos\theta_1)/c = 0.877 ,$$

$$\partial c/\partial R_2 = (R_2 - R_1\cos\theta_1)/c = 0.895 ,$$

and

$$\partial c/\partial \theta_1 = R_1R_2\sin\theta_1/c = 0.651 ,$$

and $\theta_1 = \theta_2$. Therefore,

$$0.877R_1' + 0.895R_2' + 0.651\theta_1' = 1 , \quad \text{(A4)}$$

$$0.877R_1' + 0.895R_2' + 0.651\theta_2' = 1 . \quad \text{(A5)}$$

3. *Cis*-polyacetylenes

Since $c = R_1 - R_2\cos\theta_1$, $\partial c/\partial R_1 = 1.0$, $\partial c/\partial R_2 = -\cos\theta_1 = 0.628$ and 0.621, and $\partial c/\partial \theta_1 = R_2\sin\theta_1 = 1.136$ and 1.064 for a transoidal and a cisoidal form, respectively, and $\theta_1 = \theta_2$. For a transoid form,

$$R_1' + 0.628R_2' + 1.136\theta_1' = 1 , \quad \text{(A6)}$$

$$R_1' + 0.628R_2' + 1.136\theta_2' = 1 \quad \text{(A7)}$$

and for a cisoid form,

$$R_1' + 0.621R_2' + 1.064\theta_1' = 1 , \quad \text{(A8)}$$

$$R_1' + 0.621R_2' + 1.064\theta_2' = 1 . \quad \text{(A9)}$$

[1]P. J. Barham and A. Keller, J. Polym. Sci., Polym. Lett. Ed. **17**, 591 (1962).
[2]K. Akagi, M. Suezaki, H. Shirakawa, H. Kyotani, M. Shimomura, and Y. Tanabe, Synth. Met. **28**, D1 (1989).
[3]I. Sakurada, U. Nukushina, and T. Ito, J. Polym. Sci. **57**, 651 (1962).
[4]I. Sakurada, I. Ito, and K. Nakamie, J. Polym. Sci. C **15**, 75 (1966).
[5]R. N. Britton, R. Jakeways, and I. M. Ward, J. Mater. Sci. **11**, 2057 (1976).
[6]J. Clements, R. Jakeways, and I. M. Ward, Polymer **19**, 639 (1978).
[7]R. P. Wool and R. H. Boyd, J. Appl. Phys. **51**, 5116 (1980).
[8]R. A. Feldkamp, G. Venkaterman, and J. S. King, *Neutron Inelastic Scattering* (IAEA, Vienna, 1968), Vol. II, p. 159.
[9]S. Mizushima and T. Shimanouchi, J. Am. Chem. Soc. **71**, 1320 (1949).
[10]R. F. Schaufele and T. Shimanouchi, J. Chem. Phys. **47**, 3605 (1967).
[11]G. R. Strobl and R. Eckel, J. Polym. Sci. **14**, 913 (1976).
[12]J. R. Rabolt and B. Fanconi, J. Polym. Sci. B **15**, 12 (1977).
[13]L. R. G. Treloar, Polymer **1**, 95 (1960).
[14]T. Shimanouchi, M. Asahina, and S. Enemoto, J. Polym. Sci. **59**, 93 (1962).
[15]M. Asahina and S. Enemoto, J. Polym. Sci. **59**, 101 (1962).
[16]A. Odajima and T. Maeda, J. Poly. Sci., Polym. Symp. **15**, 55 (1966).
[17]G. Wobsner and S. Blasenbrey, Kolloid Z. Z. Polym. **241**, 985 (1970).
[18]K. Tashiro, M. Kobayashi, and H. Tadokoro, Macromolecules **11**, 914 (1978).
[19]D. S. Boudreaux, J. Polym. Sci. **11**, 1285 (1973).
[20]B. Christ, M. A. Ratner, A. L. Brower, and J. R. Sabin, J. Appl. Phys. **50**, 6047 (1979).
[21]M. J. S. Dewar, Y. Yamaguchi, and S. H. Suck, Chem. Phys. **43**, 145 (1979).
[22]A. Karpfen, J. Chem. Phys. **75**, 238 (1981).
[23]S. Suhai, J. Polym. Sci., Polym. Phys. Ed. **21**, 1341 (1983).
[24]P. Pulay, in *Modern Theoretical Chemistry,* edited by H. F. Schaefer III (Plenum, New York, 1977), Vol. 4, p. 153; P. Pulay, G. Fogarasi, F. Pang, and J. E. Boggs, J. Am. Chem. Soc. **101**, 2550 (1979).
[25]P. Pulay, G. Fogarasi, G. Pongor, J. E. Boggs, and A. Vargha, J. Am. Chem. Soc. **105**, 7037 (1983); T. P. Hamilton and P. Pulay, J. Phys. Chem. **93**, 2341 (1989).
[26]A. Peluso, M. Seel, and J. Ladik, Can. J. Chem. **63**, 1553 (1985); C. X. Cui and M. Kertesz J. Chem. Phys. (to be published).
[27]M. J. S. Dewar and W. Thiel, J. Am. Chem. Soc. **99**, 4899 (1977); **99**, 4907 (1977); J. J. P. Stewart, QCPE Bull. **5**, 62 (1985); J. J. P. Stewart, *Mosol Manual,* (USAF, Colorado Springs, 1984); H. E. Klei and J. J. P. Stewart, Int. J. Quantum Chem.: Quantum Chem. Symp. **20**, 529 (1986); Y. S. Lee and M. Kertesz, J. Chem. Phys. **88**, 2609 (1988).
[28]C. W. Bunn, Trans. Faraday Soc. (London) **35**, 482 (1939).
[29]C. R. Fincher, Jr., C.-E. Chen, A. J. Heeger, A. G. MacDiarmid, and J. B. Hastings, Phys. Rev. Lett. **48**, 100 (1982).
[30]J. H. Schachtschneider and R. G. Snyder, J. Polym. Sci. C **7**, 99 (1963).
[31]H. Takeuchi, Y. Furukawa, I. Harada, and H. Shirakawa, J. Chem. Phys. **84**, 2882 (1988).
[32]M. Tasumi and T. Shimanouchi, J. Mol. Spectrosc. **9**, 261 (1962).
[33]C. X. Cui (private communication).